

## Facet Growth of $^4\text{He}$ Crystals at mK Temperatures

J. P. Ruutu,<sup>1</sup> P. J. Hakonen,<sup>1</sup> A. V. Babkin,<sup>1</sup> A. Ya. Parshin,<sup>1,2</sup> J. S. Penttilä,<sup>1</sup> J. P. Saramäki,<sup>1</sup> and G. Tvalashvili<sup>3</sup>

<sup>1</sup>*Low Temperature Laboratory, Helsinki University of Technology, FIN-02150 Espoo, Finland*

<sup>2</sup>*P. L. Kapitza Institute for Physical Problems, ul. Kosygina 2, 117334, Moscow, Russia*

<sup>3</sup>*Institute of Physics, University of Bayreuth, D-95440 Bayreuth, Germany*

(Received 30 January 1996)

We have investigated growth of  $c$  facets in good quality helium crystals with screw dislocation densities  $0\text{--}20\text{ cm}^{-2}$  along the  $c$  axis. Three distinct regimes of growth were observed. One of them can be explained by spiral growth provided that kinetic energy of moving steps and their tendency to localization at large driving forces are taken into account. In the absence of screw dislocations we find burstlike growth unless the speed is less than  $0.5\text{ nm/s}$ , in which case anomalous, intrinsic growth of facets is detected. [S0031-9007(96)00296-7]

PACS numbers: 67.80.-s, 64.70.Dv, 68.45.Da

The interface between the liquid and solid phases of helium provides a unique object to investigate interfacial physics in a situation where thermal processes do not disturb the kinetic behavior of basic surface excitations. Owing to the quantum nature of helium crystals, elementary kinks on an atomic step can be regarded as quasiparticles, moving freely along the step [1]. Highly mobile kinks and steps have provided the standard framework for theoretical description of interfacial phenomena in helium [2–4]. Typically, such a description has been very successful in explaining experimental results, e.g., crystallization waves in  $^4\text{He}$  [5]. First indications of subtle deficiencies in the standard theoretical treatment were obtained recently in high-resolution interferometric experiments performed on static properties of crystal facets [6]. In this Letter we present data which show that striking shortcomings in the theoretical understanding appear also when dynamic properties of facets are investigated.

We have studied the growth of facets in  $^4\text{He}$  crystals at mK temperatures. Typically, the growth of facets at low temperatures is assigned to the presence of screw dislocations [7,8]. Our results indicate, however, that growth is possible also in crystals with no screw dislocations at all along the  $c$  axis. In such crystals novel mechanisms are needed for growth. Our experiments show that there are two mechanisms present at low temperatures: One, continuous at small interface speeds, and another, burstlike at larger speeds. Both mechanisms are found to become increasingly effective with lowering temperature below  $0.3\text{ K}$ .

In these investigations we employed two-beam optical interferometry developed in our laboratory for experiments at ultralow temperatures [9]. In the present work, our interferometric resolution for the position of the liquid-solid interface was well below  $10\text{ nm}$ , which was obtained using the Fourier method described by Kostianovski, Lipson, and Ribak [10]. The experimental chamber was a polished copper cylinder ( $\phi = 17\text{ mm}$ , height =  $18\text{ mm}$ ) with the upper end sealed with a fused silica window whose normal is tilted by  $2^\circ$  off the cylinder axis. The lower end

was closed by a  $\text{MgF}_2$ -coated fused silica wedge acting as our optical reference flat. The cell was connected to a copper nuclear demagnetization stage via a sintered silver heat exchanger with  $100\text{ m}^2$  surface area; the total liquid volume of the setup was  $20\text{ cm}^3$ . Temperatures were measured using a Pt-wire NMR thermometer mounted on the top flange of the nuclear stage ( $T = 0.3\text{--}70\text{ mK}$ ) and with a carbon resistor located on the mixing chamber ( $20\text{--}300\text{ mK}$ ). On the basis of previous experiments by van de Haar *et al.* [11] we expect that the lowest temperatures reached in our experiments are around  $2\text{ mK}$ , although the nuclear stage was cooled down to  $0.3\text{ mK}$  in some of the runs. The basic heat leak to the nuclear stage was about  $30\text{ nW}$ . The rate of pulsed light was varied in the range of  $f = 0.01\text{--}3\text{ Hz}$  which resulted in heat leaks of  $0.02\text{--}6\text{ nW}$  to the sample owing to light absorption on the windows. Pressure was measured using a Straty-Adams type capacitive gauge having a resolution of  $0.3\text{ }\mu\text{bar}$ .

The crystals were grown using regular commercial helium with nominal purity of  $10^{-7}$ . The  $c$  facets of our crystals were aligned almost parallel to the upper surface of the optical reference wedge ( $\Delta\phi \leq 10\text{ mrad}$ ), by following the recipe described in the Ref. [12]; in these experiments, however, we did not use any high electric field to enhance the pressure locally. Our crystals were nucleated at  $20\text{ mK}$  by pressurizing the liquid slowly from a gas ballast at room temperature. First, we generated a suitable seed: the compression of the liquid was commenced  $0.8\text{ bar}$  below the melting curve which was a sufficiently low starting point so that a crystal nucleated in a quite random position on the wall at an overpressure of about  $3\text{ mbar}$ . After a few seconds the nucleated crystal either dropped to the bottom or started sliding down along the wall. By monitoring the pressure change as a function of time we could see from which height the crystal dropped. If the height was larger than  $5\text{ mm}$  and the detached crystal landed almost horizontally, the seed was regarded as suitable. By keeping the pressure thereafter within a few millibars of the melting curve, all the subsequent crystals nucleated in the same place and dropped in a similar fashion. About twenty tries

were typically sufficient to generate a crystal with a proper orientation so that interference fringes could be observed. After nucleation the crystal was grown slowly ( $1 \mu\text{m/s}$ ) across the bottom by heating a  $100 \text{ cm}^3$  gas ballast on top of the cryostat.

Growth of  $c$  facets was investigated in vertical motion at velocities  $v = 0.01 \text{ nm/s}$ – $50 \mu\text{m/s}$ . The movement of the interface could be measured either by tracing the interference lines ( $v = 0.01$ – $50 \text{ nm/s}$ ) or by using the pressure of the liquid as a level gauge ( $v = 0.05$ – $50 \mu\text{m/s}$ ). A typical  $p$  vs  $t$  plot for an advancing  $c$  facet is shown in Fig. 1(a) where the crystal is grown vertically at an average speed of  $170 \text{ nm/s}$ . The curve shows several, almost linearly increasing sections which are abruptly cut off at irregularly located points of instability. At the instability points the pressure decreases almost instantaneously down to  $100 \mu\text{bar}$  which, according to the compressibility of the liquid, corresponds to a sudden, rapid growth of the crystal by  $200$ – $2000$  layers.

During the sections of growing pressure in Fig. 1(a), there is, in fact, a slow, continuous movement of interference lines. This could be seen more reliably by stabilizing the driving pressure below the instability region. The rate for the slow growth as a function of pressure is illus-

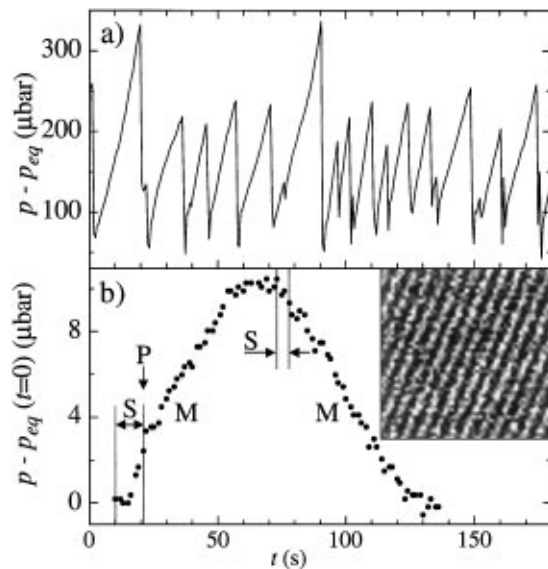


FIG. 1. (a) Deviation of pressure from equilibrium  $p - p_{eq}$  vs time  $t$  during growth ( $\langle v \rangle = 170 \text{ nm/s}$ ) of a good quality crystal, nucleated and carefully grown at  $20 \text{ mK}$ . Between the strong bursts of new atomic layers, seen as rapid drops in pressure, the  $c$  facet is growing less than two atomic layers per second. (b) Illustration of  $p - p_{eq}(t=0)$  vs  $t$  for dislocation-induced spiral growth: the crystal is grown and melted in a sinusoidal fashion using an amplitude of  $0.5 \text{ mm}$ . The regions of motion (M) and nonmotion (S) of the  $c$  facet were inferred from the movement of interference lines in small  $32 \times 32$  pixel snapshots illustrated in the inset (imaged area  $0.5 \times 0.5 \text{ mm}^2$  close to the center of the cell). The growth threshold  $\Delta p_c = 2 \mu\text{bar}$  is obtained from the extent of the stationary region (S). The traces in (a) and (b) were measured at  $T = 2$  and  $20 \text{ mK}$ , respectively.

trated in Fig. 2. The rate varies in the range  $0$ – $0.5 \text{ nm/s}$ , and it increases towards decreasing temperatures. Within our accuracy the velocity data can be fitted by a linear dependence  $v = \mu_f f$ , where  $\mu_f$  denotes the facet mobility and the driving force is defined as  $f = a(\Delta\rho/\rho_l)\Delta p$ ; here  $a = 3 \times 10^{-8} \text{ cm}$  is the interatomic spacing,  $\Delta\rho = \rho_s - \rho_l$  is the difference between solid and liquid densities, and  $\Delta p = p - p_{eq}$  denotes the pressure deviation from the equilibrium. The resulting facet mobility  $\mu_f(T)$  is illustrated in the inset of Fig. 2.

We argue that the above behavior is intrinsic for crystals without any screw dislocations along the  $c$  axis. We were able to generate screw dislocations in our experiments by growing crystals horizontally at a few hundred  $\mu\text{m/s}$  or vertically at about  $1 \mu\text{m/s}$  when  $T \sim 200 \text{ mK}$ . In the latter case, the distribution of measured instability pressures extended above  $3 \text{ mbar}$  which was a typical value for creating new crystals in our experimental chamber. According to the interference fringes, the orientation of the crystal did not change upon such an event but screw dislocations were created, which was seen as a dramatic increase in the growth rate and as a reduction of the growth threshold  $\Delta p_c$  down to about  $1 \mu\text{bar}$ . The dislocations could be eliminated by melting the crystal below its size in the original creation process.

Growth of a crystal with a small threshold is illustrated in Fig. 1(b) which displays one cycle of a sinusoidal growing and melting sequence. Initially, when helium feed to the cell is started, no growth of the facet is observed, just a gradual increase in the pressure. The growth threshold  $\Delta p_c = 2 \mu\text{bar}$  is exceeded at point P where the movement of fringes begins. The slight increase in the excess pressure ( $\sim 1 \mu\text{bar}$ ) after point P is identified as originating from the force needed to get the interface moving at the wall; this extra pressure is seen to diminish

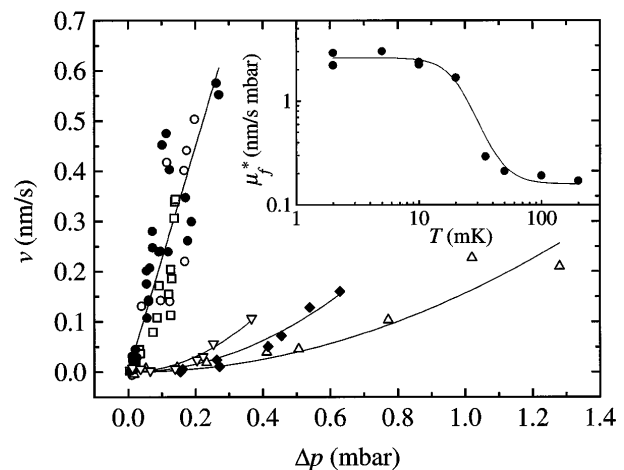


FIG. 2. Speed vs driving pressure  $\Delta p = p - p_{eq}$  for slow, intrinsic facet growth when spiral growth is absent and when bursts of new layers are avoided: ( $\circ$ )  $T = 2$ , ( $\square$ )  $10$ , ( $\bullet$ )  $20$ , ( $\nabla$ )  $50$ , ( $\blacklozenge$ )  $100$ , and ( $\triangle$ )  $200 \text{ mK}$ . The included curves are just to guide the eye. The inset shows facet mobilities obtained using linear fits,  $v = \mu_f f$ , to the data [ $\mu_f^* = a(\Delta\rho/\rho_l)\mu_f$ ].

slightly when the interface is moving. The threshold of 2  $\mu\text{bar}$  is also seen as a stationary section between growth and melting.

The growth threshold for a facet is related to the density of dislocations by the formula [4,13]  $\Delta p_c = (\rho/\Delta\rho) \times 2\beta/l$ , where  $\beta = 0.014 \text{ erg/cm}^2$  [14] is the step energy and  $l$  is the average distance between neighboring screw dislocations of different sign. Hence, our smallest growth threshold  $\Delta p_c = 0.5 \mu\text{bar}$  corresponds to a density of dislocations  $n_s = 5 \text{ cm}^{-2}$ . Our values are smaller by an order of magnitude than the previous densities reported by Lengua and Goodkind [15] and by Rolley *et al.* [14].

The velocity of *c* facets measured in a crystal with  $\Delta p_c = 0.5 \mu\text{bar}$  is displayed in Fig. 3. The data at  $T = 100, 150,$  and  $200 \text{ mK}$  can be fitted quite well by the classical  $(\Delta p)^2$  power law [4] up to velocities  $30 \mu\text{m/s}$ . At  $T = 2\text{--}20 \text{ mK}$ , on the other hand, the dependence on pressure is nearly linear within our resolution. In all sets of data, deviations from the initial pressure dependence are observed at large velocities. A hint of the physical reason for these deviations from the  $(\Delta p)^2$  power law can be obtained from the estimation of the step velocity  $v_s$ . This speed is related to the facet velocity by the formula  $v = (a/d)v_s$ , where  $d$  is the spacing of the spiral arms. Using  $\Delta p = 2 \mu\text{bar}$ ,  $v = 10 \mu\text{m/s}$ , and  $d \approx 20(\rho/\Delta\rho)\beta/\Delta p$  (valid for classical spiral growth) we obtain  $v_s = 300 \text{ m/s}$ , i.e., a value which equals the sound velocity in helium. At such large velocities the standard theory of spiral growth [4] is not sufficient and modifications of the calculation are needed.

In our modified theory of spiral growth two new features have been taken into account: step inertia and localization of steps at large driving forces. The equation of step motion can be written in the form

$$m(\partial v_s/\partial t + v_s \partial v_s/\partial n) = f - \beta^* a/\tilde{r} - v_s/\mu, \quad (1)$$

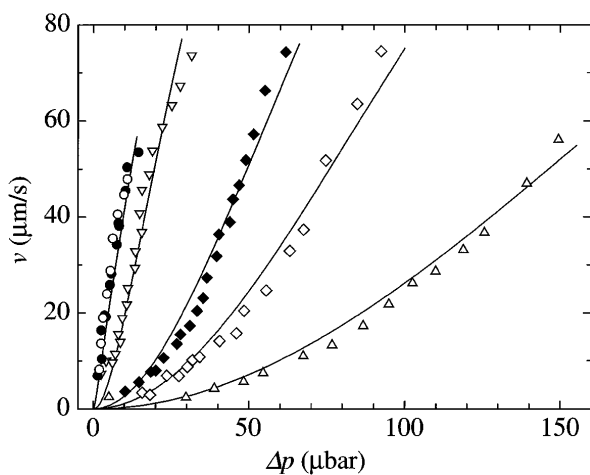


FIG. 3. Facet velocity  $v$  as a function of driving pressure  $\Delta p$  for a crystal with dislocation density  $n_s = 5 \text{ cm}^{-2}$  ( $\Delta p_c = 0.5 \mu\text{bar}$ ): (○)  $T = 2$ , (●) 20, (▽) 50, (◆) 100, (◇) 150, and (△) 200 mK. The fitted solid curves are discussed in the text.

where  $m$  is the effective mass of a step per unit length,  $n$  is normal to the step,  $\beta^* a = \beta a + mv_s^2/2$  denotes the step energy including the kinetic energy,  $\tilde{r}$  is the radius of curvature of the step at a given point, and  $\mu$  is the step mobility. Stationary solutions of Eq. (1), corresponding to growth of the whole facet with constant velocity  $v$ , were obtained numerically.

At low temperatures, where the mobility of steps is large,  $v_s = \mu f$  as before, but the asymptotic spacing of the spiral arms  $d = \pi\mu(2ma\beta)^{1/2}$  differs from its classical value, which leads to a linear velocity versus pressure dependence as seen in the experiments. From the data in this limit we may estimate the step mass  $m = (4 - 5) \times 10^{-18} \text{ g/cm}$  which is in a good agreement with the theoretical value [3,16]  $m = (5 - 7) \times 10^{-18}$ . At higher temperatures, Eq. (1) yields the regular  $(\Delta p)^2$  dependence.

In the “inertial” limit ( $\mu \rightarrow \infty$ ) with constant values of  $m$  and  $\beta$ , Eq. (1) predicts a temperature independent velocity  $v$ . However, the experimental values of  $v$  in Fig. 3 decrease significantly at higher temperatures. In addition, the measured velocities display a tendency to saturation above  $40 \mu\text{m/s}$ . This can be viewed as an indication of localization under large driving forces [17]. Such a behavior is expected for quantum systems with narrow-band quasiparticles, like kinks on a step [1]. As long as kink movement implies the motion of steps, localization of kinks might result in localization of the step itself. In the regime of localization, the speed of a step is inversely proportional to the driving pressure and the mobility can be expressed as

$$1/\mu = 1/\mu_0 + \eta f^2, \quad (2)$$

where  $\mu_0$  is the step mobility at small speeds and  $\eta$  is a parameter describing energy relaxation of “localized” steps. Fitting of this formula to the experimental data in the range  $T = 50\text{--}200 \text{ mK}$  yields a temperature independent value  $\eta = 3 \times 10^2$ ; at low temperatures  $T = 2\text{--}20 \text{ mK}$  a reasonable agreement is also obtained with this value. Solid lines in Fig. 3 illustrate the good quality of our theoretical fits for spiral growth obtained with Eqs. (1) and (2) using the step mobility  $\mu_0$  as a fitting parameter at constant  $\eta = 3 \times 10^2$  and  $m = 5 \times 10^{-18} \text{ g/cm}$ .

Temperature variation of the burstlike growth mechanism without screw dislocations is illustrated in Fig. 4 which displays cumulative distributions of instability pressures at three different temperatures. These distributions were measured at an average interfacial velocity of  $200\text{--}300 \text{ nm/s}$  but no variation as a function of speed was observed in the range  $100\text{--}600 \text{ nm/s}$ . With increasing temperature the asymmetry of the distributions about their median values becomes more prominent. In general, the functional shapes agree with expectations for thermal and quantum tunneling [18].

The inset of Fig. 4 displays the temperature dependence of the median pressures taken from the measured distributions. There is an increase by a factor of 3 in the median pressure when  $T$  is increased from 20 to 200 mK; i.e.,

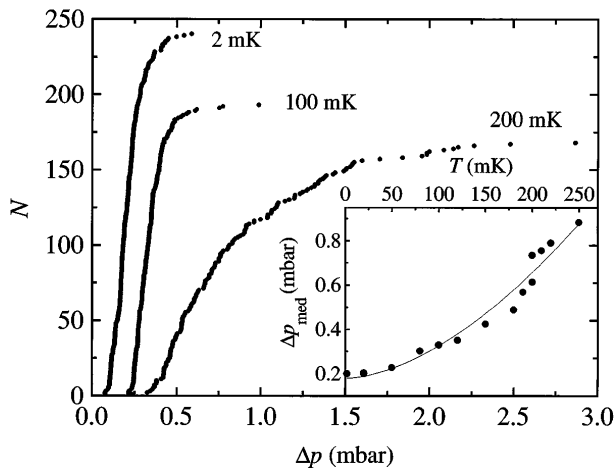


FIG. 4. Cumulative distribution of pressure jumps in the burst growth [see Fig. 1(a)] measured at an average velocity 200–300 nm/s;  $N$  denotes the number of nucleation events below the pressure  $p = p_{\text{eq}} + \Delta p$ . The median value of the distributions  $\Delta p_{\text{med}}$  vs  $T$  is displayed in the inset.

there is a clear decrease in the average growth rate with increasing temperature. Above 200 mK, we were not able to obtain good statistics since the pressurization quickly resulted in the destruction of this growth mode by the creation of screw dislocations.

In order to check the role of  $^3\text{He}$  impurities, which are known to have a bound state at the liquid/solid interface [19], we added 2.5 cm<sup>3</sup> of  $^3\text{He}$  gas (*NTP*) to the ballast volume and drove the impurities to the experimental region by growing and melting the crystal repeatedly (the original seed was kept unchanged). We relied on the fact that the heat flush effect should transport  $^3\text{He}$  atoms quite effectively to the experimental region once they entered the superfluid. After adding  $^3\text{He}$ , the average pressure became approximately 2 times larger in the burstlike growth and the rate for the slow intrinsic growth decreased by a factor of 3. Hence, we may conclude that the presence of an enhanced amount of impurities is detrimental for the growth processes in the absence of screw dislocations.

In conclusion, we have shown that it is possible to generate very good crystals by nucleation at 20 mK in the absence of pressure gradients. We have identified three different regimes for crystal growth at ultralow temperatures. One of them can be assigned to the screw-dislocation-mediated spiral growth provided that inertial and localization effects are taken into account. In the absence of screw dislocations, facet growth is typically made of consecutive jumps whose occurrence in pressure displays a strongly temperature dependent distribution. At small speeds up to 0.5 nm/s, we observe anomalous, slow facet growth, approximately linearly dependent on the driving pressure.

We want to thank A. Andreev, S. Balibar, O. Lounasmaa, M. Paalanen, and E. Rolley for useful discussions

and correspondence. This work was supported by the Academy of Finland and by the Human Capital and Mobility Program ULTI of the European Community.

- [1] A. F. Andreev and A. Ya. Parshin, *Zh. Eksp. Teor. Fiz.* **75**, 1511 (1978) [*Sov. Phys. JETP* **48**, 763 (1978)].
- [2] K. O. Keshishev, A. Ya. Parshin, and A. I. Shal'nikov, *Soviet Scientific Reviews, Section A: Physics Reviews*, edited by I. M. Khalatnikov (Harwood Academic, New York, 1982), Vol. 4, p. 155.
- [3] P. Nozières and M. Uwaha, *J. Phys. (Paris)* **48**, 389 (1987).
- [4] P. Nozières, in *Solids Far From Equilibrium*, edited by C. Godrèche (Cambridge University Press, Cambridge, 1991), p. 1.
- [5] O. A. Andreeva, K. O. Keshishev, A. B. Kogan, and A. N. Marchenkov, *Europhys. Lett.* **19**, 683 (1992); C. L. Wang and G. Agnolet, *Phys. Rev. Lett.* **69**, 2102 (1992); E. Rolley, E. Chevalier, C. Guthmann, and S. Balibar, *Phys. Rev. Lett.* **72**, 872 (1994).
- [6] A. V. Babkin, H. Alles, P. J. Hakonen, A. Ya. Parshin, J. P. Ruutu, and J. P. Saramäki, *Phys. Rev. Lett.* **75**, 3324 (1995).
- [7] P. E. Wolf, F. Gallet, S. Balibar, E. Rolley, and P. Nozières, *J. Phys. (Paris)* **46**, 1987 (1985).
- [8] V. L. Tsymbalenko, *Fiz. Nizk. Temp.* **21**, 162 (1995) [*Sov. J. Low Temp. Phys.* **21**, 120 (1995)].
- [9] A. J. Manninen, J. P. Pekola, G. M. Kira, J. P. Ruutu, A. V. Babkin, H. Alles, and O. V. Lounasmaa, *Phys. Rev. Lett.* **69**, 2392 (1992); H. Alles, J. P. Ruutu, A. V. Babkin, P. J. Hakonen, O. V. Lounasmaa, and E. B. Sonin, *Phys. Rev. Lett.* **74**, 2744 (1995).
- [10] S. Kostianovski, S. G. Lipson, and E. N. Ribak, *Appl. Opt.* **32**, 4744 (1993).
- [11] See, e.g., P. G. van de Haar, C. M. C. van Woerkens, M. W. Meisel, and G. Frossati, *J. Low Temp. Phys.* **86**, 349 (1992).
- [12] A. V. Babkin, D. B. Kopeliovich, and A. Ya. Parshin, *Zh. Eksp. Teor. Fiz.* **89**, 2288 (1985) [*Sov. Phys. JETP* **62**, 1322 (1985)].
- [13] M. Uwaha and P. Nozières, *J. Phys. (Paris)* **48**, 407 (1987).
- [14] E. Rolley, C. Guthmann, E. Chevalier, and S. Balibar, *J. Low Temp. Phys.* **99**, 851 (1995).
- [15] G. A. Lengua and J. M. Goodkind, *J. Low Temp. Phys.* **79**, 251 (1990).
- [16] A. M. Kosevich and Yu. A. Kosevich, *Fiz. Nizk. Temp.* **7**, 809 (1981) [*Sov. J. Low Temp. Phys.* **7**, 394 (1981)].
- [17] See, e.g., L. Esaki, *Phys. Scr.* **T42**, 102 (1992), and references therein.
- [18] J. P. Ruutu *et al.* (to be published).
- [19] Y. Carmi, E. Polturak, and S. G. Lipson, *Phys. Rev. Lett.* **62**, 1364 (1989); C. L. Wang and G. Agnolet, *J. Low Temp. Phys.* **89**, 759 (1992); E. Rolley, S. Balibar, C. Guthmann, and P. Nozières, *Physica (Amsterdam)* **210B**, 397 (1995).